JACS
JOURNAL OF THE AMERICAN CHEMICAL SOCIETY

Communication

pubs.acs.org/JACS

Size-Dependent Electrophoretic Deposition of Catalytic Gold Nanoparticles

Rafael A. Masitas,[†] Stacy L. Allen,[‡] and Francis P. Zamborini*[,‡]

[†]Department of Chemistry & Biochemistry, University of Notre Dame, Notre Dame, Indiana 46556, United States
[‡]Department of Chemistry, University of Louisville, Louisville, Kentucky 40292, United States

Supporting Information

ABSTRACT: Here we describe size-dependent electrophoretic deposition (EPD) of citrate-stabilized Au nanoparticles (NPs) onto indium-tin-oxide-coated glass (glass/ITO) electrodes as studied by linear sweep stripping voltammetry (LSSV) and scanning electron microscopy (SEM). LSSV allows both the determination of the Au NP coverage and NP size from the peak area and the peak potential, respectively. Two-electrode EPD in aqueous solutions of Au NPs plus H_2O_2 reveal that a minimum potential of 1.5 V is needed for significant deposition of 4 nm diameter Au NPs as opposed to 2.0 V for 33 nm diameter Au NPs. EPD at 0.4 V in a solution of Au NPs prepared with a short 5 min reaction time led to the successful capture of 1−2 nm diameter Au NPs with appreciable coverage. In all cases, deposition did not occur in the absence of H_2O_2. Three-electrode experiments with a real reference electrode revealed the same size selective deposition with potential and that the amount of Au deposited depends on the deposition time and H_2O_2 concentration. The deposition occurs indirectly by oxidation of H_2O_2, which liberates protons and neutralizes the citrate stabilizer, leading to precipitation of the Au NPs onto the glass/ITO electrode. Studies on pH stability show that larger Au NPs aggregate at lower pH compared to smaller Au NPs. More importantly, though, 4 nm diameter Au NPs are much more catalytic for H_2O_2 oxidation, which is the main reason for the size selective deposition.

The assembly of metallic or semiconductor nanostructures on solid surfaces is of tremendous interest in many areas of science and technology due to the important applications of nanostructures in sensing, optical, electronic, photovoltaic, biomedical, and catalytic devices. Many assembly methods exist, including drop-cast deposition,[1] chemical assembly,[2] and electrophoretic deposition.[1,3−5]

In the case of negatively charged, citrate-coated Au nanoparticles (NPs), as described here, most assembly methods employ chemical attachment to thiol (SH)-functionalized surfaces or electrostatic attachment to positively charged amines ($-NH_3^+$). In this type of approach, the particle transport is governed solely by Brownian motion, resulting in completely random particle-particle and particle-substrate collisions. Also, the size and shape of deposited nanostructures is not selective if the solution contains particles with large dispersity. Electrophoretic deposition (EPD) is an alternative assembly method previously employed to deposit metallic,[6,7] semiconducting,[8] and insulating[9] nanoparticles on conductive substrates.

Several studies explored the EPD of Au NPs. For example, Giersig and Mulvaney prepared highly ordered 2D films of Au NPs from aqueous and organic media onto transmission electron microscopy (TEM) grids by EPD.[7,10] Bailey et al. prepared patterned thin films of colloidal Au by EPD.[6] The applied electric field drove the movement of the colloidal Au NPs from the solution to the surface of the substrate.[6] Kooij et al. studied the potential dependence on the electric-field assisted deposition of 8.6 nm diameter, positively charged Au NPs by spectroscopic ellipsometry.[11] At a threshold voltage, electrochemical reduction at the working electrode created a net space charge, which created an electric field extending through the cell, driving the movement and deposition of the charged Au NPs.[11] Buttard et al. studied EPD of colloidal Au NPs on a silicon wafer by scanning electron microscopy (SEM).[12] They found a dense and uniform distribution of NPs with no aggregation over the surface.[12]

Interestingly, none of these previous reports closely examined the dependence of Au NP size on EPD and while deposition is thought to be electric-field driven, the detailed mechanism and the NP-substrate interaction is not well understood. Our goal was to use EPD to deposit selectively small Au NPs in the presence of a disperse population with larger Au NPs as a potential method for preparing small metal NPs supported on electrode surfaces for electrocatalytic applications. Because the electrophoretic mobility of ions or particles increases with increasing charge/size ratio, we hypothesized that smaller Au NPs would have a higher mobility and deposit more readily at lower voltages, allowing for size selectivity. Because our synthesis of larger Au NPs involved H_2O_2, we instead accidentally discovered that H_2O_2 plays a key role in the EPD of citrate-coated Au NPs and can allow size selectivity in the deposition, not because of differences in electrophoretic mobility but because of differences in electrocatalytic activity for H_2O_2 oxidation. An important aspect of this work is that we directly analyzed the size and coverage of the Au NPs deposited by EPD by monitoring the peak potential of oxidation (E_p) and the peak area in a linear sweep stripping voltammogram (LSSV) of the electrode/Au NP assembly. Our previous work showed that the E_p for Au oxidation in bromide solutions strongly depends on size from 1 to 50 nm, which allowed for the fast analysis of the EPD process and its mechanism.[1,2,13]

Received: September 1, 2016
Published: November 2, 2016

DOI: 10.1021/jacs.6b09172
J. Am. Chem. Soc. 2016, 138, 15295−15298

We synthesized 33, 17, 4, and <4 nm diameter citrate-coated Au NPs in solution, added equal amounts of H_2O_2 to each solution, and performed EPD by applying a positive voltage to a glass/ITO electrode relative to a second Au foil electrode in a two-electrode cell setup (Scheme S1A of SI). We also studied the deposition mechanism with 4, 15, and 50 nm diameter citrate-coated Au NPs with H_2O_2 added in a three-electrode cell setup (Scheme S1B of SI). We measured the size and coverage of the Au NPs on the electrodes after EPD by LSSV in a similar manner as described in our previous studies.[1,2,13,14] All experimental details are in the SI. Figure 1A shows LSSVs of glass/ITO

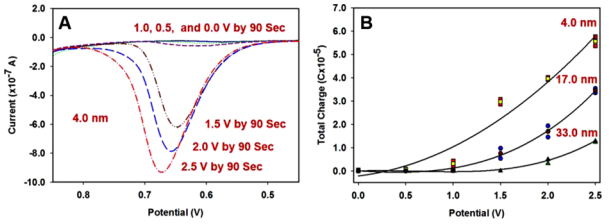

Figure 1. (A) LSSV of glass/ITO electrodes in 0.1 M $HClO_4$ + 0.01 M KBr at a scan rate of 0.001 V/s after EPD of 4 nm diameter citrate-coated Au NPs at 2.5, 2.0, 1.5, 1.0, 0.5, and 0.0 V for 90 s as indicated. (B) Average coverage of Au (n = 3) based on the integration of the LSSV peak as a function of EPD potential for 4, 17, and 33 nm diameter Au NPs.

electrodes after EPD using the two-electrode setup at different potentials in a solution containing 4 nm diameter citrate-coated Au NPs and H_2O_2. The peak at 0.65−0.70 V corresponds to the bromide-induced oxidation and dissolution of 4 nm diameter Au NPs attached to the electrode. The presence of this peak after EPD at 2.5, 2.0, and 1.5 V for 90 s shows that the 4 nm diameter Au NPs deposited on the glass/ITO at all of these potentials. In contrast, a very small or no peak in this region after EPD at 1.0, 0.5, and 0.0 V for 90 s shows little or no deposition at these lower voltages. Additional LSSVs for 4 and 33 nm Au NPs are presented in Figure S1 of SI. Figure 1B shows a plot of the Au coverage as a function of EPD potential for 4, 17, and 33 nm diameter Au NPs after doing the same experiment shown in Figure 1A. All 3 sizes deposited significantly at 2.5 V for 90 s. At 1.5 V, both 4 and 17 nm diameter Au NPs deposited on the electrode, but the 33 nm diameter Au NPs showed no significant deposition. At 1.0 V, only the 4 nm diameter Au NPs deposited to a significant extent. At 0.5 V or below, no deposition occurred with any of the Au NPs significantly. In this way, the EPD potential acts as a low pass filter for depositing Au NPs of a certain size or smaller onto the electrode surface. We note that potentials of 1.5 V or higher would likely be sufficient to form a surface Au oxide on the NPs during deposition, but we did not analyze the Au surface for the presence of oxide.

Figure 2A shows LSSVs of a glass/ITO electrode after EPD at different potentials from a mixture of 4 and 33 nm diameter citrate-coated Au NPs containing 6.5×10^{-6} M and 13×10^{-6} M Au, respectively, plus equal amounts of H_2O_2. After EPD at 2.5 V for 90 s, we observed stripping peaks for both the 33 and 4 nm Au NPs as labeled in Figure 2, indicating they both deposited onto glass/ITO during EPD. The coverage in terms of total Au is slightly higher for the 33 nm Au NPs as expected based on the amount of Au in each NP solution. At 2.0 V, we still observed stripping peaks for both 33 and 4 nm diameter Au NPs, but the coverage in terms of total Au was lower for the 33 nm Au NPs compared to 4 nm Au NPs. At 1.5 V, there was only one peak for

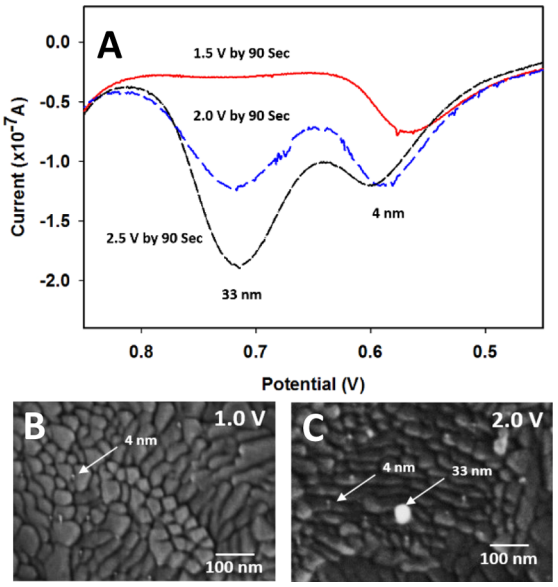

Figure 2. (A) LSSVs of glass/ITO electrodes in 0.1 M $HClO_4$ + 0.01 M KBr at a scan rate of 0.001 V/s after EPD from a mixed solution of 33 and 4 nm Au NPs for the indicated potential and time. Panels B and C show SEM images after EPD at the indicated potentials.

the 4 nm diameter Au NPs, showing its selective deposition over larger 33 nm Au NPs by EPD. Figure 2B,C shows corresponding SEM images of glass/ITO electrodes after EPD of the mixture of 4 and 33 nm Au NPs at 1.0 and 2.0 V. Both 4 and 33 nm diameter Au NPs appear on the surface after EPD at 2.0 V, but only 4 nm diameter Au NPs appear after EPD at 1.0 V. The presence of 33 nm diameter Au NPs was not detected in the LSSV at 1.5 V (Figure 2A), but some did deposit based on SEM (Figure S2 of SI). The 33 nm Au NPs did not deposit at 1.0 V based on LSSV or SEM.

Interestingly, we discovered that H_2O_2 is a critical component for EPD of the Au NPs to occur. Figure S3 shows LSSVs of glass/ITO following EPD of citrate-coated 4 nm diameter Au NPs at 1.5 V for 90 s in the presence and absence of H_2O_2. The LSSV shows a clear Au stripping peak at 647 mV after EPD in the presence of H_2O_2 but no peak after EPD in the absence of H_2O_2, showing that H_2O_2 plays an important role in the EPD process and likely the size selection.

A real reference electrode was necessary to determine if the Au NP deposition coincided with the oxidation or reduction of H_2O_2. In these experiments, we varied the amount of H_2O_2, the EPD voltage, and the time of EPD for 4, 15, and 50 nm diameter Au NPs. The amount of Au deposited depended on the deposition time and H_2O_2 concentration as shown in Figures S4 and S5 of SI. These studies were performed to optimize the amount of H_2O_2 and the time for the size-dependent studies. The deposition amount was maximum for a EPD solution containing 5 mL Au solution, 10 mL water, and 5 mL 30% H_2O_2. Because 10 mL of 30% H_2O_2 did not lead to a significant difference in Au NP coverage for a 1.0 V potential and 30 s time of deposition, we used 5 mL for all subsequent studies.

Figure 3 shows LSSVs of glass/ITO electrodes after EPD of 4, 15, and 50 nm diameter Au NPs with a constant amount of water, constant concentration of total Au (6.2×10^{-5} M), and a varying EPD potential. The amount of H_2O_2 was constant for 4 and 15 nm diameter Au NPs, but about double that for the 50 nm Au NPs because H_2O_2 was used in the synthesis. A similar potential-dependent deposition of the different sized Au NPs occurred as

DOI: 10.1021/jacs.6b09172
J. Am. Chem. Soc. 2016, 138, 15295−15298

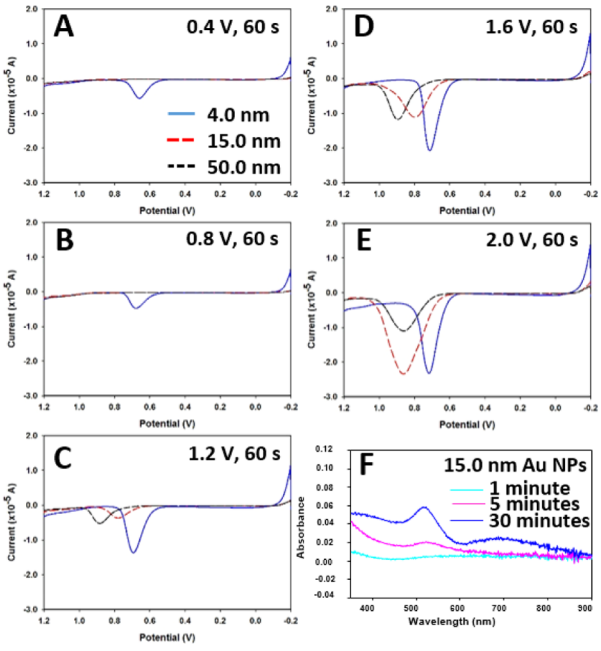

Figure 3. (A–E) LSSVs of glass/ITO performed in 0.1 M $HClO_4$ + 0.01 M KBr at a scan rate 0.01 V/s after EPD of 4, 15, and 50 nm citrate-coated Au NPs for 60 s at (A) 0.4 V, (B) 0.8 V, (C) 1.2 Vs, (D) 1.6 V, and (E) 2.0 V. (F) UV–vis spectra of glass/ITO after EPD of 15 nm Au NPs.

in the two-electrode studies, but at slightly different potentials due to the use of a real reference electrode. In this case, 4 nm diameter Au NPs started to deposit at 0.4 V, whereas 15 nm diameter Au NPs and 50 nm diameter Au NPs started to deposit at 1.2 V. It is therefore difficult to select between the 15 and 50 nm diameter Au NPs, but easy to separate out the smaller 4 nm diameter Au NPs from larger sizes. Additionally, Figure 3F shows UV–vis spectra of glass/ITO electrodes after EPD with constant H_2O_2 and water, constant concentration of Au, and varying deposition time for 15 nm diameter Au NPs. The absorbance increases with time in good agreement with our LSSV studies shown in Figure S4 of SI.

We hypothesized that EPD occurs indirectly by oxidation of H_2O_2 to form H^+ ions, which causes a drop in pH near the electrode, leading to Au NP deposition through neutralization of the stabilizing citrate anions. The oxidation of H_2O_2 occurs as follows.

$$H_2O_2 \rightleftarrows O_2 + 2H^+ + 2e^- \quad E^0 = 0.682 \text{ vs NHE}$$

This proposed EPD mechanism is shown in Scheme S2 of SI. To provide support for this mechanism, we obtained linear sweep voltammograms (LSVs) in a solution of H_2O_2 in water, H_2O_2 plus citrate in water, and 4 nm diameter citrate-coated Au NPs with H_2O_2 in water from −0.2 to +1.2 V at a scan rate of 0.01 V/s using a three-electrode cell, where the working electrode was bare glass/ITO, the counter electrode was a Pt wire, and the reference electrode was Ag/AgCl (3 M KCl). Figure 4A shows the LSVs in these three solutions. With H_2O_2 only, the current is very low at all potentials, mainly due to the high solution resistance (no added electrolyte) and large overpotential for H_2O_2 oxidation on glass/ITO. With H_2O_2 and citrate added, some H_2O_2 oxidation occurred near 0.8 V, but the current is still very small due to high overpotential. With H_2O_2, citrate, and 4 nm diameter Au NPs, H_2O_2 oxidation occurs significantly near 0.5 V and the current is much larger at potentials beyond. The

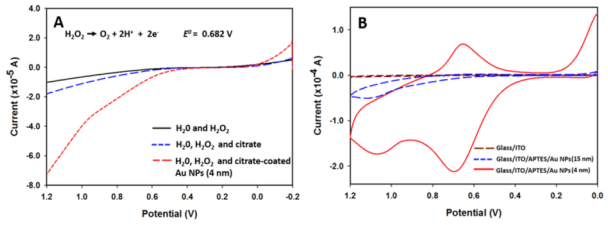

Figure 4. (A) LSVs of glass/ITO in H_2O, H_2O_2, and 4 nm Au NPs (red dashed plot), H_2O, H_2O_2 and citrate (blue dashed plot), and H_2O and H_2O_2 (black solid plot) performed at a scan rate of 0.01 V/s. (B) CVs of glass/ITO (brown dashed plot), glass/ITO/APTES/Au NPs (15 nm) (blue dashed plot), and glass/ITO/APTES/Au NPs (4 nm) (red solid plot) in 0.1 M $KClO_4$ + 0.25 mM H_2O_2 at 0.05 V/s.

current is larger and the potential for H_2O_2 oxidation is smaller due to the 4 nm diameter Au NPs catalyzing H_2O_2 oxidation. We postulate that the catalytic H_2O_2 oxidation at the surface of the 4 nm diameter Au NPs leads to H^+ formation, which causes neutralization of the negative charge of the citrate-coated Au NPs. As a consequence of the neutralization, the NPs lose stability and precipitate (deposit) on the glass/ITO surface. Because the potentials are fairly high in some of the EPD experiments, it is not clear if the deposited Au NPs have an oxide layer or not.

Figure 4A clearly shows larger currents for H_2O_2 oxidation with Au NPs in solution, which likely leads to the deposition, but does not explain the size selectivity. We postulated that size selectivity must be due to either (1) different pH stability or (2) different electrocatalytic activity of the different sized Au NPs. To test the first possibility, we monitored the pH-induced aggregation of 4, 15, and 50 nm diameter Au NPs in solutions optically. As shown in Figure S6, the red color of the stable Au NPs turned blue at pH 2.92, 2.63, and 1.91 for the 4, 15, and 50 nm diameter Au NPs, respectively. This shows that larger Au NPs are more stable at low pH, which could possibly explain why a more positive potential is needed to deposit them. We also attached 4 and 15 nm diameter Au NPs electrostatically to glass/ITO electrodes functionalized with amino-propyltriethoxysilane (APTES) and obtained cyclic voltammograms (CVs) in H_2O_2 solution to determine if they have different electrocatalytic activity for H_2O_2 oxidation. Figure 4B shows CVs for glass/ITO, glass/ITO/APTES/$AuNP_{15\ nm}$, and glass/ITO/APTES/$AuNP_{4\ nm}$ working electrodes in a solution of 0.25 mM H_2O_2 plus 0.1 M $KClO_4$. There is no noticeable current on the glass/ITO electrode, a small current on the glass/ITO/APTES/$AuNP_{15\ nm}$ electrode starting at about 0.8 V, and a very large current on glass/ITO/APTES/$AuNP_{4\ nm}$ starting at about 0.5 V. The lower overpotential and larger current shows a much higher activity for H_2O_2 oxidation at 4 nm diameter Au NPs relative to 15 nm diameter Au NPs. This is likely the main reason for the selective deposition of 4 nm diameter Au NPs over 15 nm and larger Au NPs, although the pH stability may also play a role. The H_2O_2 oxidation potentials observed in the voltammetry are consistent with the EPD potentials for the different sized Au NPs, showing a strong likelihood that the proposed mechanism is correct. Other studies have also stated that liberation of H^+ or OH^- in aqueous solutions at positive and negative potentials, respectively, is responsible for EPD of negatively- and positively-charged particles, respectively.[15]

One of our initial goals that inspired this research was to use EPD to deposit very small, highly catalytic metal nanostructures with a high coverage from a solution that may also contain larger

DOI: 10.1021/jacs.6b09172
J. Am. Chem. Soc. 2016, 138, 15295–15298

NPs with low catalytic activity. In Figure 5, we used EPD to attach citrate-coated Au NPs <4 nm

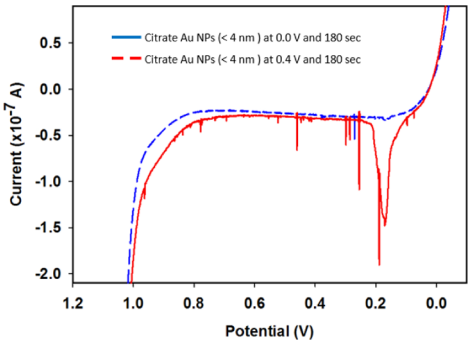

Figure 5. LSSVs of glass/ITO electrodes from −0.1 to +1.2 V at 0.001 V/s obtained in 0.1 M $HClO_4$ + 0.01 M KBr following EPD of <4 nm diameter Au NPs at 0.0 V for 180 s (blue plot) and 0.4 V for 180 s (red plot).

diameter citrate-coated Au NPs was performed as reported previously by our group[1] using borohydride reduction of $AuCl_4^-$ in the presence of citrate with a reaction time of 5 min instead of the standard 2 h reaction time, which normally produces 4 nm diameter Au NPs. At this short reaction time, small Au NPs are in solution since the reaction is still in the early stages of the nucleation and growth process. Performing size-selective EPD could potentially allow attachment of these small Au NPs to electrode surfaces preferentially over the larger Au NPs. Figure 5 shows the LSSV obtained in 0.01 M KBr plus 0.1 M $HClO_4$ on a glass/ITO electrode after EPD at 0.4 V for 180 s in a solution of Au NPs (formed after 5 min reaction) plus H_2O_2. The LSSV has one oxidation peak at 180 mV whereas the LSSV for 4 nm Au NPs prepared by reduction for 2 h (Figure 3) only exhibits one main peak near 700 mV with no discernible peaks at the lower potentials. We also performed a LSSV plot for a control sample where we applied 0.0 V for 180 s to a solution of Au NPs prepared the same way (5 min reaction time) and we did not observe any significant peaks at all in the LSSV. This result suggests that a combination of short reaction time during synthesis and EPD at low voltage is a useful method for attaching very small metal NPs to an electrode support. An additional benefit is that these Au NPs are citrate-coated, which is a weak stabilizer and unlikely to inhibit the catalytic reactivity of the metal surface. An oxidation potential of 180 mV correlates to Au NPs below 2 nm in diameter according to our earlier work and the theory developed by Plieth.[16]

In summary, we have reported the size selective electrochemical deposition of citrate-coated Au NPs on glass/ITO in the presence of H_2O_2. The data suggest that the generation of H^+ at the electrode by oxidation of H_2O_2 leads to neutralization of citrate and NP deposition. In this work, 4 nm diameter Au NPs were more electrocatalytic compared to 15 nm and larger Au NPs, leading to preferential deposition and easy size selection with potential. A low deposition potential of 0.4 V in a solution of Au NPs synthesized for a short time (5 min) allowed the EPD of Au NPs < 2 nm, which could be applicable to the selective attachment of small, highly active electrocatalysts on porous electrode supports. Future studies will examine the effect of electrolyte, ionic strength, and pH on EPD as well as other H^+ and non-H^+ generating redox active molecules to study the role of other forces that may affect the size-selective deposition process, such as electrophoretic mobility, surface forces, and hydrodynamic drag near the electrode. This work is relevant to not only NP electrocatalysis studies but also NP collision studies at microelectrodes because size selective responses and NP deposition during NP-electrode collisions are important issues.[17,18]

■ ASSOCIATED CONTENT

Supporting Information

The Supporting Information is available free of charge on the ACS Publications website at DOI: 10.1021/jacs.6b09172.

Experimental details for chemical synthesis of citrate-coated Au NPs, EPD, and LSSV and SEM characterization, schemes for the deposition procedure with a two- and three-electrode cell, influence of H_2O_2 concentration and time during deposition, SEM of 4 nm and 33 nm citrate-coated Au NPs at different EPD voltage, and pH stability of the citrate-coated Au NPs (PDF)

■ AUTHOR INFORMATION

Corresponding Author

*f.zamborini@louisville.edu

Notes

The authors declare no competing financial interest.

■ ACKNOWLEDGMENTS

We gratefully acknowledge the National Science Foundation (CHE-1308763 and CHE-1611170) for financial support of this research. Thanks to Keith Stevenson for helpful discussions about the deposition mechanism.

■ REFERENCES

(1) Masitas, R. A.; Khachian, I. V.; Bill, B. L.; Zamborini, F. P. *Langmuir* **2014**, *30*, 13075.
(2) Masitas, R. A.; Zamborini, F. P. *J. Am. Chem. Soc.* **2012**, *134*, 5014.
(3) Shortell, M. P.; Liu, H.-W.; Zhu, H.; Jaatinen, E. A.; Waclawik, E. R. *Langmuir* **2010**, *26*, 14472.
(4) Sahoo, S.; Husale, S.; Karna, S.; Nayak, S. K.; Ajayan, P. M. *J. Am. Chem. Soc.* **2011**, *133*, 4005.
(5) Brown, P.; Kamat, P. V. *J. Am. Chem. Soc.* **2008**, *130*, 8890.
(6) Bailey, R.; Stevenson, K. J.; Hupp, J. *Adv. Mater.* **2000**, *12*, 1930.
(7) Giersig, M.; Mulvaney, P. *J. Phys. Chem.* **1993**, *97*, 6334.
(8) Salant, A.; Shalom, M.; Hod, I.; Faust, A.; Zaban, A.; Banin, U. *ACS Nano* **2010**, *4*, 5962.
(9) Cihlar, J.; Drdlik, D.; Cihlarova, Z.; Hadraba, H. *J. Eur. Ceram. Soc.* **2013**, *33*, 1885.
(10) Giersig, M.; Mulvaney, P. *Langmuir* **1993**, *9*, 3408.
(11) Kooij, E.; Brouwer, E.; Poelsema, B. *J. Electroanal. Chem.* **2007**, *611*, 208.
(12) Buttard, D.; Oelher, F.; David, T. *Nanoscale Res. Lett.* **2011**, *6*, 580.
(13) Ivanova, O. S.; Zamborini, F. P. *J. Am. Chem. Soc.* **2010**, *132*, 70.
(14) Ivanova, O. S.; Zamborini, F. P. *Anal. Chem.* **2010**, *82*, 5844.
(15) Besra, L.; Uchikoshi, T.; Suzuki, T. S.; Sakka, Y. *J. Eur. Ceram. Soc.* **2010**, *30*, 1187.
(16) Plieth, W. J. *J. Phys. Chem.* **1982**, *86*, 3166.
(17) Dasari, R.; Robinson, D. A.; Stevenson, K. J. *J. Am. Chem. Soc.* **2013**, *135*, 570.
(18) Zhou, H.; Fan, F.-R. F.; Bard, A. J. *J. Phys. Chem. Lett.* **2010**, *1*, 2671.

DOI: 10.1021/jacs.6b09172
J. Am. Chem. Soc. 2016, 138, 15295−15298